Carbohydrate Polymers 76 (2009) 509–512

Contents lists available at ScienceDirect

Carbohydrate Polymers

journal homepage: www.elsevier.com/locate/carbpol

In situ synthesis of CdS nanoparticles on bacterial cellulose nanofibers

Xin Li, Shiyan Chen *, Weili Hu, Shuaike Shi, Wei Shen, Xiang Zhang, Huaping Wang *

State Key Laboratory for Modification of Chemical Fibers and Polymer Materials, Key Laboratory of Textile Science and Technology (Ministry of Education), College of Materials Science and Engineering, Donghua University, Shanghai 201620, PR China

ARTICLE INFO

Article history:
Received 6 August 2008
Received in revised form 6 November 2008
Accepted 10 November 2008
Available online 20 November 2008

Keywords:
Bacterial cellulose
CdS nanoparticles
Nanocomposite

ABSTRACT

CdS nanoparticles have been synthesized and stabilized on unique bacterial cellulose (BC) nanofibers in situ. The obtained nanocomposite material have been characterized by scanning electron microscopy (SEM), X-ray diffraction (XRD), fourier transformed infrared (FTIR), thermogravimetric analysis (TGA), ultraviolet–visible (UV–Vis) and photoluminescence (PL) spectroscopy. The results indicated that CdS nanoparticles of about 30 nm diameter deposited on BC nanofibres are well-dispersed in the BC nanofibre-network and the uniform spherical CdS nanoparticles are comprised of nano-sized CdS crystal. Moreover, the crystallite sizes of CdS crystals are about 8 nm. The nanocomposites would have potential application as photocatalyst, novel luminescence and photoelectron transfer devices.

1. Introduction

Bacterial cellulose obtained through fermentation by the acetobacter xylinum is of great interest because of its unique specific structure and properties. It presents unique properties and structures such as high Young's modulus of 138 GPa, the tensile strength of at least 2 GPa, high purity (free of lignin and hemicelluloses), high crystallinity and good biocompatibility, ultra fine three dimensional (3D) network with a distinct tunnel and pore structure, well-separated nano- and microfibrils creating an extensive surface area. Current applications for bacterial cellulose include use as materials for industry (paper, headphone membranes, food and textiles) and use as biomaterials including temporary skin substitute, artificial blood vessels (Czaja, Young, Kawecki, & Brown, 2007; Kamel, 2007). In addition to these applications, there is also an important application for BC in terms of its unique nano- and microfibrils 3D network. It serves as a template or matrix for synthesis of nanoparticles, nanowires (Barud et al., 2008; Maneerung, Tokura, & Rujiravanit, 2008; Zhang & Qi, 2005).

Quantum dot (QD)-CdS, as typical II–VI semiconductor nanoparticles have received much interest in terms of their unique optical properties, photocatalytic and tunable photoluminescence (Niemeyer, 2003). For device fabrication CdS nanoparticles is required to be embedded into a matrix. Polymers are considered to be a good matrix. Till now many polymer matrix has been used to fabricate CdS/polymer nanocomposite such as silk fibroin, polyacrylamide, etc. (Pardo-Yissar, Bourenko, Wasserman, & Willner, 2002; Su, Han, Dong, Zhang, & Guo, 2008).

In fact, well-separated nano- and microfibrils of BC create an extensive surface area which is very helpful for its adsorption of metal ion (Chen et al., 2009). The extensive surface area means BC has much more surface hydroxyl and ether groups than other cellulose. These hydroxyl groups make up of active sites for metal ion adsorption. So it is feasible for BC to serve as an excellent matrix in the synthesis of CdS nanoparticles in situ. In this paper, we firstly fabricate CdS/BC nanocomposite using in situ method. At first, hydroxyl and ether groups of BC anchored Cd^{2+}, then anchored Cd^{2+} reacted with S^{2-} in situ successively to generate CdS nanoparticles on the BC nanofibers. The distribution of CdS nanoparticles in the BC is expected to be homogeneous throughout the whole BC volume. Incorporation CdS nanoparticles into BC will form an important luminescent nanocomposite materials because this material integrate BC's excellent properties and CdS luminescent properties.

2. Experimental

2.1. Materials and instruments

All chemicals were used as received without any further purification. High purity Millipore water was used in all experiments.

The infrared spectra of BC, Cd^{2+}–BC membrane complexes and CdS/BC nanocomposite were recorded on a Nicolet NEXUS-670 FTIR. The sample was grounded with dried potassium bromide (KBr) powder and compressed into a disc, and then was subjected to analysis. XRD measurements were performed. XRD patterns were obtained in a Rigaku D/max-2000 X-ray diffractometer with a thin-film attachment with the Cu Ka radiation ($k = 1.54056$ Å) at a scanning rate of 2°/s ranging from 4° to 70° (2θ angle). Prior

* Corresponding authors. Tel.: +86 21 67792958; fax: +86 21 67792726.
E-mail addresses: chensy@dhu.edu.cn (S. Chen), wanghp@dhu.edu.cn (H. Wang).

0144-8617/$ - see front matter © 2008 Elsevier Ltd. All rights reserved.
doi:10.1016/j.carbpol.2008.11.014

to SEM analysis, samples cut from the freeze–dried CdS/BC composite were coated with gold palladium by cathodic spreading using a PolaronE 5100 coater. The images were taken using JEOL, JSM-5600LV SEM with an accelerating voltage of 15 kV. TG was performed under nitrogen atmosphere using a Netzsch TG 209 F1 with a heating rate of 20 °C/min. PL spectra were measured on a JASCO FP-6600 spectrofluorometer.

2.2. Synthesis and purification of BC membranes

The bacteria strain gluconoacetobacter xylinus was incubated for 10 days in a static culture namely Hestrin–Schramm culture medium (HS) (2.5 w/v% D-glucose, 0.5 w/v% peptone, 0.5 w/v% yeast extract, 0.115 w/v% citric acid, and 0.25 w/v% disodium hydrogen phosphate) at 28 °C. The pH of the HS culture medium was adjusted to 6.0. The obtained membranes were boiled in 1 wt% NaOH solution. After that, the BC pellicles were washed with pure water sufficiently till the filtrate became neutral.

2.3. In situ synthesis of CdS nanoparticles on the BC nanofibers

In a typical procedure, the purified BC membranes were immersed into a beaker containing 10 mL 1 mM aqueous solution of $Cd(NO_3)_2{\cdot}5H_2O$ for 3 days, allowing sufficient time to reach equilibrium swelling. Then they were taken out and rinsed with pure water several times. Finally, it was immersed into a 10 mL 1 mM aqueous solution of Na_2S for 1 min. Then it was observed that the BC membranes changed to a yellowish color (not the solution).

3. Results and discussion

3.1. Formation of CdS nanoparticles on BC fibers

Cd^{2+} were first anchored on some BC fibers through ion–dipole interactions (Shim et al., 2001) during the soaking of BC in $Cd(NO_3)_2$ solution. After being rinsed sufficiently with pure water to remove the unanchored Cd^{2+}, performed Cd^{2+}/BC complexes are immersed into the Na_2S solution. The interaction between the Cd^{2+} and S^{2-} was immediate, and it was obvious by the appearance of a yellow color, which is associated only with the BC and does not extend over the solution.

3.2. FTIR characterization

In order to reveal the reactive site during in situ synthesis and examine the interaction between CdS nanoparticles and BC, FTIR measurements were performed. Fig. 1 shows the FTIR spectra of the BC, Cd^{2+}/BC and CdS/BC composite. It can be seen that after dipping BC into $Cd(NO_3)_2$ solution, the peaks at 3410 cm^{-1} corresponding to stretching vibrations of hydroxyl groups of BC moves noticeably to lower wavenumbers (3350 cm^{-1}). After forming CdS nanoparticles on the BC also stretching vibrations of hydroxyl groups of BC moves noticeably to lower wavenumbers (3290 cm^{-1}). The result indicates that the hydroxyl groups are the active cites during in situ synthesis and a strong interaction between this group and CdS nanoparticles. At the same time, the peaks at 1420 and 1068 cm^{-1}, assigned to the symmetric bending of CH_2 and C_3–O stretching, respectively, also moved to higher wavenumbers, which also indicated the interaction between cellulose chain and CdS nanoparticles.

3.3. SEM and XRD analysis

To confirm the formation of CdS nanoparticles on the BC nanofibers, the samples were analyzed with a scanning electron microscope. From Fig. 2a we can see the 3D porous network structure of BC membrane and the nanofibers (20–80 nm) clearly. This exquisite structure gives a good tunnel for Cd^{2+} adsorption and makes Cd^{2+} homogeneously distributed on the BC nanofibers. Fig. 2b shows the SEM image of CdS nanoparticles onto the BC nanofibers. We can see that nanoparticles with a size of about 30 nm were well-dispersed in the BC. The crystallographic nature of the nanoparticles on BC was further investigated by X-ray diffraction. From XRD shown in Fig. 3, we can find broad diffraction peaks at about 14.6° and 22.8°, which are assigned to the crystallographic plane of $(1\bar{1}0)$ and (200) reflection of BC, respectively (Tokoh, Takabe, Fujita, & Saiki, 1998). Apart from the diffraction peaks of BC, there are additional peaks in the CdS/BC nanocomposite. Three broad but distinct peaks displayed at 2θ values of 26.6°, 44.1°, and 52.0° are assigned to (111), (220), and (311) crystalline planes of cubic CdS, respectively, indicating the formation of CdS in the BC matrix. It can be seen that CdS in the BC matrix prefers cubic structure. This evidence confirmed that nanoparticles formed on the surface of BC fibers correspond to CdS nanoparticles.

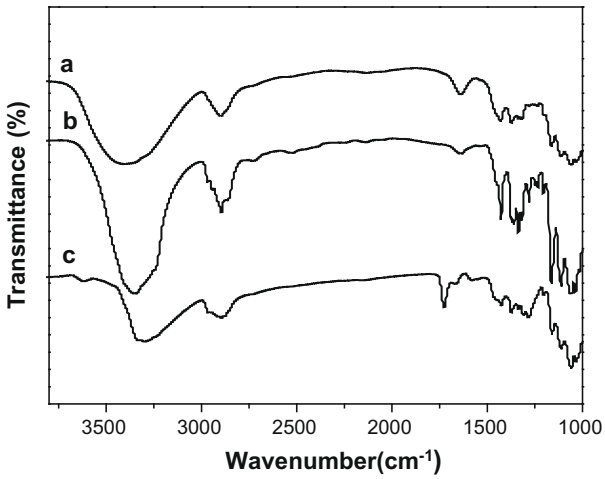

Fig. 1. FTIR of BC (a), as-dipped BC in $Cd(NO_3)_2$ solution (b) and re-dipped BC into Na_2S solution (C), respectively.

3.4. Thermal properties

Fig. 4 shows the TG curves of pure BC and CdS/BC nanocomposite. As shown in Fig. 4a two significant weight loss platforms are observed from ambient to 300 °C and from 300 to 400 °C. The first significant weight loss is due to BC dehydration. Physically absorbed and hydrogen bonded linked water molecules can be lost at this stage. The other stage corresponding to a broad peak (300–400 °C) can be attributed to BC pyrolysis. Fig. 4b shows the TG curve of CdS/BC nanocomposite. Comparing with that of BC, we can see inclusion of CdS nanoparticles into BC in situ improved the thermal stability of BC. This also indicated there is an interaction between BC and CdS nanoparticles.

3.5. UV–Vis and PL properties

Fig. 5 illustrates the UV–Vis absorption spectrum of CdS/BC nanocomposite and the PL spectra of BC and CdS/BC nanocomposite at room temperature with an excitation wavelength at 370 nm. As seen in Fig. 5a, a significant absorption of UV light at 426 nm was observed with a 90 nm blue-shift when compared with the characteristic absorption of the corresponding band gap of bulk CdS (515 nm), reflecting the quantum confinement effect of the CdS nanocrystal (Hwang et al., 2006). The PL spectrum of

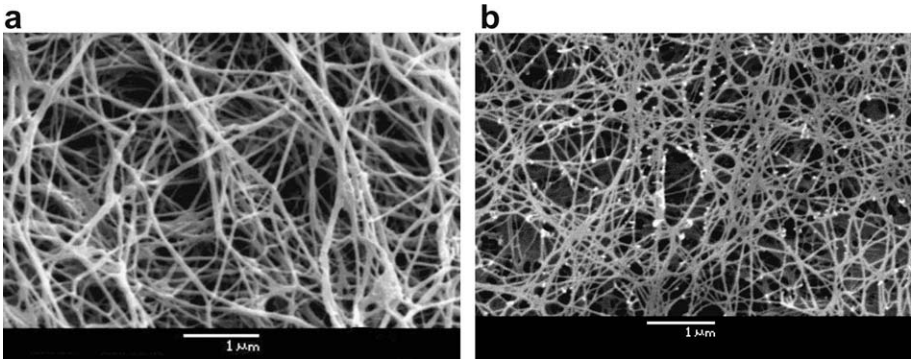

Fig. 2. SEM images of BC (a) and CdS/BC nanocomposite (b).

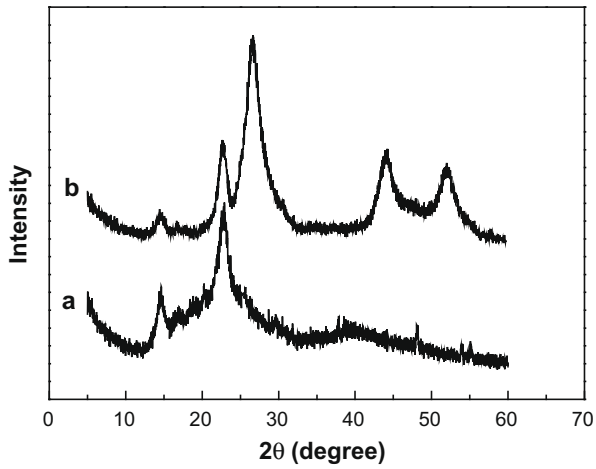

Fig. 3. XRD patterns of BC (a) and CdS/BC nanocomposite (b).

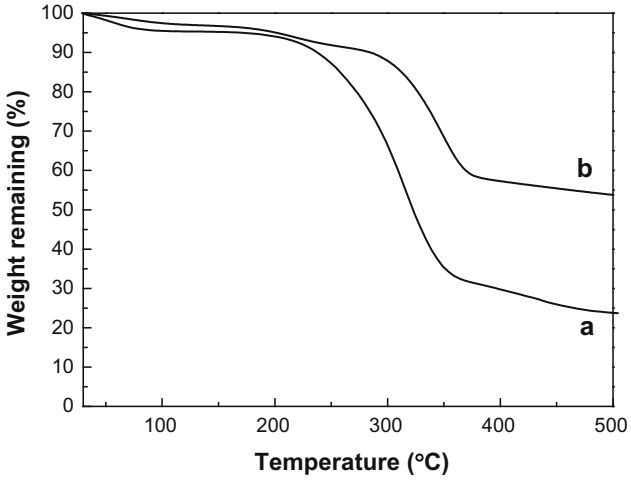

Fig. 4. TG curves of BC (a) and CdS/BC nanocomposite (b).

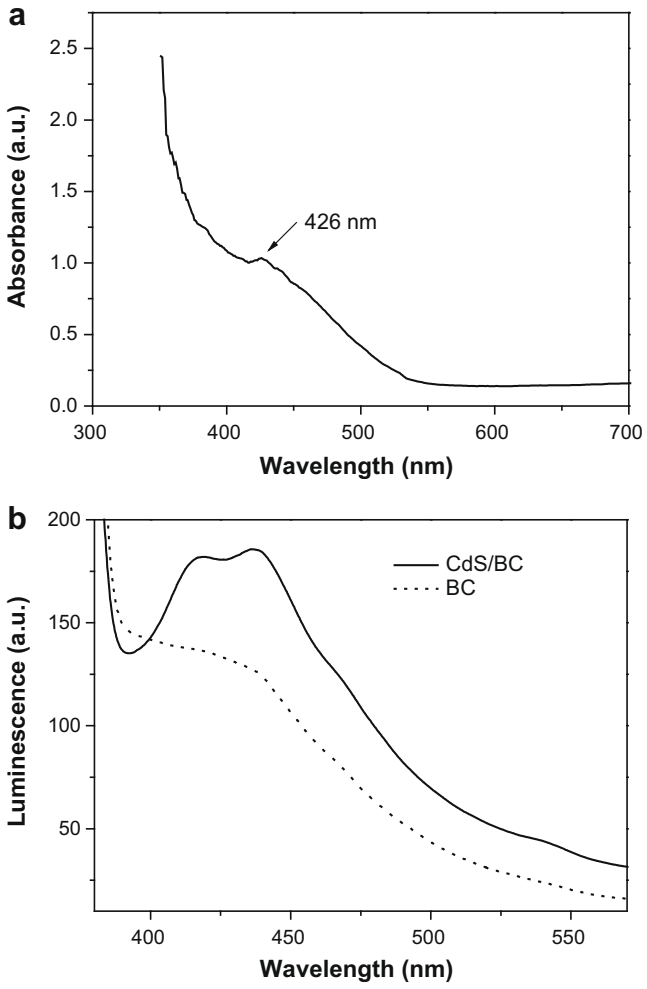

Fig. 5. (a) UV–Vis absorption spectrum of CdS/BC nanocomposite and (b) PL spectra of BC and CdS/BC nanocomposite with excitation wavelength at 370 nm.

CdS/BC nanocomposite is shown in Fig. 5b. Compared with the original BC, there are two emission peaks at 417 and 437 nm which blue-shifts about 60 nm from that of CdS bulk materials. The result is in accord with the previously reported result (Liu et al., 2006). The emission can be attributed to a high level transition in CdS semiconductor crystallites, which arise from the recombination of excitons and/or shallowly trapped electron–hole pairs (Zhan et al., 2000).

4. Conclusion

To summarize, we succeeded in the synthesis of CdS nanoparticles on the BC nanofibers. The unique structure and the ether and hydroxyl groups of bacterial cellulose nanofibers constitute an effective nanoreactor for in situ synthesis of CdS nanoparticles. This technique could be extended to the growth of other type of crystals such as AgCl, ZnS. The ether oxygen and the hydroxyl group not only anchor Cd^{2+} tightly on the BC nanofibers via ion–dipole interactions, but also stabilize CdS nanoparticles by strong

interaction with their surface hydroxyl groups. The XRD and SEM analysis indicated that well-dispersed CdS nanoparticles on the BC nanofibers. More than that, inclusion of CdS into BC improved its thermal stablility. Further investigation such as variation the immersing time or solution concentration is in progress.

Acknowledgments

This work was financially supported by Programme of Introducing Talents of Discipline to Universities (111-2-04, B07024), New Century Excellent Talents in University (NCET-05-0420) and Shanghai Leading Academic Discipline Project (B603).

References

Barud, H. S., Barrios, C., Regiani, T., Marques, R. F. C., Verelst, M., DexpertGhys, J., et al. (2008). Self-supported silver nanoparticles containing bacterial cellulose membranes. *Materials Science and Engineering: C, 28*, 515–518.

Chen, S., Zou, Y., Yan, Z., Shen, W., Shi, S., Zhang, X., et al. (2009). Carboxymethylated-bacterial cellulose for copper and lead ion removal. *Journal of Hazardous Materials, 161*, 1355–1359.

Czaja, W. K., Young, D. J., Kawecki, M., & Brown, R. M. (2007). The future prospects of microbial cellulose in biomedical applications. *Biomacromolecules, 8*, 1–12.

Hwang, S.-H., Moorefield, C. N., Wang, P., Jeong, K.-U., Cheng, S. Z. D., Kotta, K. K., et al. (2006). Construction of CdS quantum dots via a regioselective dendritic functionalized cellulose template. *Chemical Communications*, 3495–3497.

Kamel, S. (2007). Nanotechnology and its applications in lignocellulosic composites, a mini review. *eXPRESS Polymer Letters, 1*, 546–575.

Liu, W., He, W., Zhang, Z., Zheng, C., Li, J., Jiang, H., et al. (2006). Fabrication of CdS nanorods in inverse microemulsion using HEC as a template by a convenient g-irradiation technique. *Journal of Crystal Growth, 290*, 592–596.

Maneerung, T., Tokura, S., & Rujiravanit, R. (2008). Impregnation of silver nanoparticles into bacterial cellulose for antimicrobial wound dressing. *Carbohydrate Polymers, 72*, 43–51.

Niemeyer, C. M. (2003). Functional hybrid devices of proteins and inorganic nanoparticles. *Angewandte Chemie International Edition, 42*, 5796–5800.

Pardo-Yissar, V., Bourenko, T., Wasserman, J., & Willner, I. (2002). Solvent-switchable photoelectrochemistry in the presence of CdS-Nanoparticle/acrylamide hydrogels. *Advanced Materials, 14*, 670–673.

Shim, I.-W., Choi, S., Noh, W.-T., Kwon, J., Cho, J. Y., Chae, D.-Y., et al. (2001). Preparation of copper nanoparticles in cellulose acetate polymer and the reaction chemistry of copper complexes in the polymer. *Bulletin of the Korean Chemical Society, 22*, 772–774.

Su, H., Han, J., Dong, Q., Zhang, D., & Guo, Q. (2008). In situ synthesis and photoluminescence of QD-CdS on silk fibroin fibers at room temperature. *Nanotechnology, 19*, 025601.

Tokoh, C., Takabe, K., Fujita, M., & Saiki, H. (1998). Cellulose synthesized by Acetobacter xylinum in the presence of acetyl glucomannan. *Cellulose, 5*, 249–261.

Zhan, J. H., Yang, X. G., Wang, D. W., Li, S. D., Xie, Y., Xia, Y., et al. (2000). Polymer-controlled growth of CdS nanowires. *Advanced Materials, 12*, 1348–1351.

Zhang, D., & Qi, L. (2005). Synthesis of mesoporous titania networks consisting of anatase nanowires by templating of bacterial cellulose membranes. *Chemical Communication*, 2735–2737.